



# Hydrogen/deuterium exchange of phenylalanine analogs studied with infrared multiple photon dissociation

Cesar S. Contreras<sup>a,1</sup>, Nicolas C. Polfer<sup>a</sup>, Alfred C. Chung<sup>b</sup>, Jos Oomens<sup>c</sup>, John R. Eyler<sup>a,\*</sup>

<sup>a</sup> Department of Chemistry, University of Florida, P.O. Box 117200, Gainesville, FL 32611-7200, USA

<sup>b</sup> Interdisciplinary Center for Biotechnology Research, Proteomics Division, University of Florida, Gainesville, FL, USA

<sup>c</sup> FOM-Institute for Plasma Physics Rijnhuizen, Nieuwegein, The Netherlands

## ARTICLE INFO

### Article history:

Received 11 May 2010

Received in revised form 18 August 2010

Accepted 19 August 2010

Available online 6 September 2010

### Keywords:

FTICR

Amino acids

IRMPD

Ab initio

Hydrogen–deuterium exchange

Phenylalanine

## ABSTRACT

Phenylalanine analogs were subjected to hydrogen/deuterium exchange (HDX) in both solution and the gas phase, and gas-phase infrared multiple photon dissociation spectra were obtained for each of the species. For sodium cation-attached N-acetylphenylalanine, gas-phase HDX took place at only one site. Comparison of spectra from both undeuterated and singly deuterated sodiated N-acetylphenylalanine showed band shifts for normal modes that involved mainly vibrations of the O–H group, indicating that gas-phase exchange occurs at the COOH hydrogen and not at the NH hydrogen. Conversely, HDX in solution did result in exchange of the NH hydrogen, even for the protected species O-methyl N-acetylphenylalanine and N-acetylphenylalanine O-methylglycine. Rate coefficients for gas-phase H/D exchange were measured for the single deuteration of sodiated N-acetylphenylalanine and all three deuterations of protonated N-acetylphenylalanine, and found to be in the range  $(1.5\text{--}3.6) \times 10^{-11} \text{ cm}^3/\text{s}$ .

Density functional theory calculations predicted that the phenylalanine analogs, although of different size, have relatively similar structural features. These calculations showed that  $\text{Na}^+$  interacts with the phenyl ring and all available carbonyl oxygens, thus essentially locking the structures into one basic conformation. This behavior is quite distinct from other amino acids which are more flexible, and where gas-phase exchange also occurs at the amine (NH) group.

© 2010 Elsevier B.V. All rights reserved.

## 1. Introduction

Hydrogen deuterium exchange (HDX) is a method in which particularly labile hydrogen atoms are substituted with deuterium atoms in a molecule or ion of interest [1–8]. H/D exchange has been used in solution-phase studies to obtain structural information for large biomolecules using both mass spectrometric [5,8,9] and nuclear magnetic resonance (NMR) [10] techniques. H/D exchange studies have also been conducted in the gas phase and early mass spectrometric work from Beauchamp et al. probed the proton affinity and exchange rates of labile hydrogen atoms [11], while ion–molecule reactions involving H/D exchange have also been followed in mass spectrometry experiments [12]. Utilizing the technique of infrared multiple photon dissociation (IRMPD) [13–18], infrared spectra of gas-phase deuterated ions can be obtained, and these have recently been used to obtain structural information for small ions [19–27] and biologically relevant ions

[28–30], occasionally observing the spectral shifts that occur in the infrared spectra due to deuteration [31].

H/D exchange experiments can provide a great deal of structural information, especially when coupled with mass spectrometric and/or infrared spectral techniques. Substitution of hydrogen by deuterium has primarily been used to obtain information on the tertiary structure of proteins [9], but can also provide primary structural information for smaller species such as the phenylalanine analogs studied in this work. In the case of amino acids, exchange is seen for hydrogen atoms bound to the Lewis base oxygen and nitrogen atoms [32].

Phenylalanine (Phe), one of the essential amino acids, has been studied extensively both in solution and in the gas phase [30,33–39]. Recent work has shown that Phe behaves differently in each phase, in part due to structural differences of the molecule in the two phases [40]. The binding of alkali metals to Phe in the gas phase has been especially well characterized [35–37]. However, much less is known of the effect that protecting groups or modifications to the amino acid have on the phenylalanine structure. Recent work by Dunbar and co-workers [30] showed that when the backbone is extended, e.g., by forming a dipeptide, an attached alkali cation has a higher possibility of forming a chelating

\* Corresponding author. Tel.: +1 352 392 0532; fax: +1 352 392 0872.

E-mail address: [eylerjr@chem.ufl.edu](mailto:eylerjr@chem.ufl.edu) (J.R. Eyler).

<sup>1</sup> Present address: NASA Ames Research Center, Moffett Field, CA, USA.

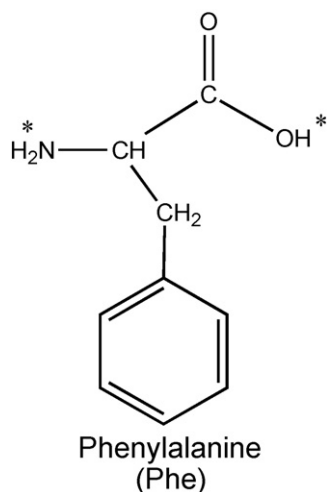


Fig. 1. Phenylalanine structure with exchangeable hydrogens indicated by asterisks.

complex. The sodium cation tends to interact with electronegative sites on the extended chain, subject to steric hindrance constraints. For sodiated PheAla and AlaPhe, the most energetically favorable structures involve a sodium cation– $\pi$  interaction with the phenyl ring. The phenylalanine moiety tends to pucker to allow the alkali metal to interact with both the phenyl ring and the lone-pair electrons on the oxygen or nitrogen atoms. To further investigate the effect that modification of phenylalanine has on the chelating complexes, in the work reported here phenylalanine analogs bound to a sodium cation were studied in the gas phase after either solution- or gas-phase HDX.

In this work a sodium cation was attached to each phenylalanine analog in solution, and the resulting charged complexes were desolvated during the electrospray ionization process [41–43] to produce isolated ions. Infrared multiple photon dissociation spectra of the Phe analogs cationized by sodium then provided structural information, when combined with theoretical calculations. Density functional theory (DFT) [44–46] calculations were used to predict the lowest energy structures of each analog.

Neutral Phe has three potential hydrogen atoms which can undergo H/D exchange (Fig. 1). Limiting the deuteration sites to one or two positions, by the addition of protecting groups, allows observed spectral shifts to be clearly defined and simplifies band assignment and subsequent structure elucidation. The analogs of Phe studied in this work had protecting groups on all but one or two of the possible exchange sites. The analogs, N-acetylphenylalanine (AcPhe), O-methyl N-acetylphenylalanine (AcPheOMe) and N-acetylphenylalanine O-methylglycine (AcPheGlyOMe) are shown in Fig. 2. AcPhe has two exchangeable hydrogen atoms (in the COOH and NH groups), AcPheOMe has one, and AcPheGlyOMe has two.

## 2. Materials and methods

### 2.1. Sample preparation

Phe analogs were synthesized from a commercial sample of L-phenylalanine (Sigma–Aldrich Co.) at the Proteomics Division of the Interdisciplinary Center for Biotechnology Research at the University of Florida. Stock solutions were made by dissolving 0.01 g/mL of the analogs in an 80:20  $\text{CH}_3\text{OH}:\text{H}_2\text{O}$  mixture.

For solution-phase HDX, a solution of 80:20  $\text{CH}_3\text{OD}:\text{D}_2\text{O}$  was used to dilute the stock sample to 1 mM, and an equimolar amount of NaCl was added. Samples were allowed to undergo solution-phase HDX for a minimum of 20 min followed by electrospray ionization.

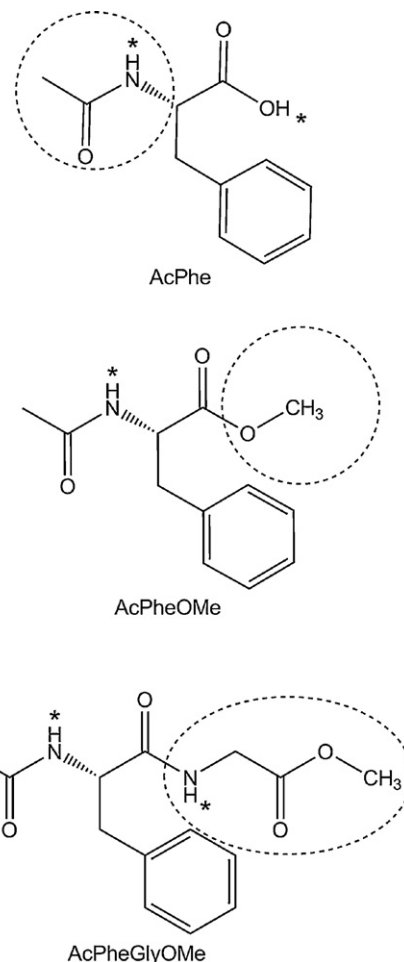


Fig. 2. Phe analogs studied in this work. The portion encircled by dashed lines represents the N-acetyl adduct in AcPhe, the methyl group in AcPheOMe, and the O-methylated glycine in AcPheGlyOMe, respectively. Exchangeable hydrogen atoms are indicated by asterisks.

### 2.2. Instrumentation

Electrospray ionization was conducted with a Z-spray source (Micromass/Waters Corporation, Milford, MA) at a solution flow rate of 20  $\mu\text{L}/\text{min}$ , with the flow rates of the nebulizing gas and the desolvation gas ( $\text{N}_2$ ) set to 32 and 150 L/h, respectively, and the electrospray needle voltage set at 3 kV. A 4.7 T superconducting magnet (Cryomagnetics Inc., Oak Ridge, TN) was used with a laboratory-constructed pumping system, ion trap and electronics console. The Fourier transform ion cyclotron resonance (FTICR) mass spectrometer has been described previously [23]. Precursor ions were isolated using the stored waveform inverse Fourier transform (SWIFT) [47–51] technique to eject all unwanted ions. Ions were detected using the broadband detection mode. For the IRMPD activation, the Free Electron Laser for Infrared eXperiments (FELIX) [52,53] was used with the wavelength scanned over the range of 5.5–12.5  $\mu\text{m}$  ( $1800\text{--}800\text{ cm}^{-1}$ ). Mass-selected precursor ions were irradiated in the open cylindrical FTICR ion trap for a period of 4 s at each wavelength with an average power of 50–60 mJ per macropulse and a laser repetition rate of 5 macropulses per second. Typically, four individual transients were accumulated at each wavelength to improve the signal-to-noise ratio. The intensities of the precursor ion and the product ions produced from it by the IRMPD process were monitored throughout the experiment. The IRMPD yield at a given frequency is calculated from the measured intensities of the precursor and product ions,  $I_{\text{prec}}$  and  $I_{\text{prod}}$ , respec-

tively, corrected for the frequency dependent laser power  $P(\omega)$ .

$$\text{IRMPD yield} = (P(\omega))^{-1} \times \frac{(\sum I_{\text{prod}})}{(I_{\text{prec}} + \sum I_{\text{prod}})}$$

For gas-phase HDX,  $\text{ND}_3$  was introduced into the ICR vacuum chamber at a background pressure of  $3 \times 10^{-7}$  torr, and allowed to react with the cationized Phe analogs for 1–5 s after which mass isolation and laser irradiation were applied. For species where no gas-phase exchange was detected, reaction time was increased up to 35 s to verify that no reaction had taken place.

In order to minimize back exchange, the instrument was passivated with  $\text{ND}_3$  for at least an hour prior to either monitoring the results of solution-phase HDX experiments or following the results of gas-phase HDX.

### 2.3. Computational

The Hyperchem suite of programs [54] was used to assign trial structures to the phenylalanine analogs. Depending on the analog, methyl or acetyl groups were added to a core Phe structure to produce trial AcPhe, AcPheOMe and AcPheGlyOMe structures. Sodium was initially placed near the carboxyl or carbonyl group of the Phe analogs, and the complex was given an overall charge of +1. It should be noted that although the sodium was placed near the carboxyl or carbonyl group, the mere electrostatic interaction allowed sodium to freely move during the geometry optimization. The dihedral angles which were varied in the conformational search were explicitly defined and are shown in Fig. 3 [55,56].

Using the usage directed approach [57], 1000 structures were generated using the semi-empirical AM1 level of theory embedded in the Hyperchem software to probe the conformational space of each analog. During the conformational search, the algorithm can eliminate duplicate structures, comparing energies, torsion angles, and RMS fit residual errors in position between corresponding atoms in the molecular reference frame. The comparison threshold values were set to 0.05 kcal/mol,  $10^\circ$  and 0.25 Å, respectively. All conformers within 15 kcal/mol of the lowest energy conformer were further refined by geometry optimization using Gaussian03 [58] at the B3LYP/6-31G(d) level of theory [59,60]. The B3LYP hybrid functional was used since it has been shown to be adequate for predicting infrared spectra of Phe in earlier studies [30,39]. The conformations were compared and duplicate conformations having the same energy (within 0.0001 hartree), and the same vibrational spectrum as the comparison conformer were discarded. Using the B3LYP/6-311++G(d,p) level of theory [61,62], an average of 45 conformers were further geometry optimized, and a vibrational frequency calculation, at the same level of theory, was performed for each of these conformations. The calculated frequencies were scaled by 0.965, followed by comparison to experimental spectra.

## 3. Results and discussion

### 3.1. N-acetylphenylalanine

Calculated infrared spectra for the four lowest energy conformers (Fig. 4) of sodiated AcPhe are compared to the experimental IRMPD spectrum obtained for this complex in Fig. 5. Conformer A has a cation- $\pi$  interaction (Fig. 4) while conformer B does not, although the conformers have virtually equal energies with a difference of only 0.04 kcal/mol with conformer A being the lowest energy structure. The calculated spectrum of conformer B gives a poorer match to the experimental data relative to that of conformer

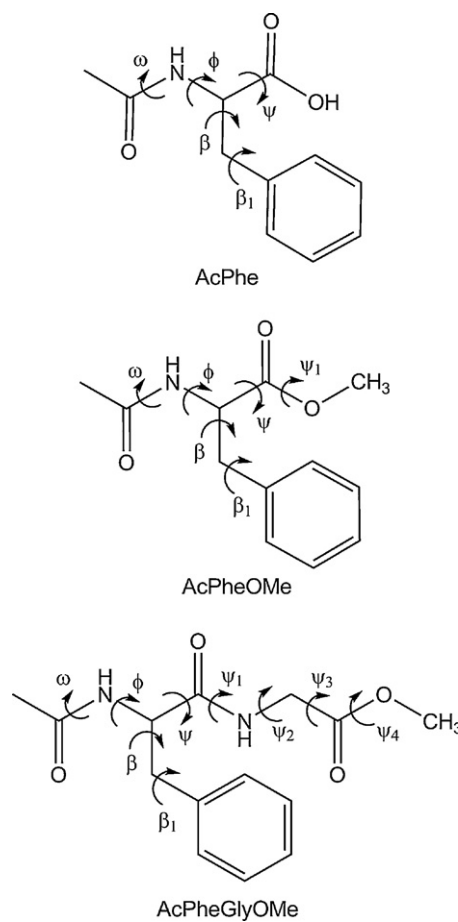


**Fig. 3.** Dihedral angles (shown with arrows) defined for the conformational search calculations of AcPhe, AcPheOMe and AcPheGlyOMe. The labeling scheme for the dihedral angles is similar to that of Momany et al. and Dunfield et al. [55,56].

A. When compared to the experimental C=O stretching bands ( $1660$  and  $1720\text{ cm}^{-1}$ ), the calculated C=O stretches for conformer B are red shifted. The interaction between the sodium cation and the carbonyl groups is stronger since the cation- $\pi$  interaction does not occur in conformer B. The C=O stretch frequencies of conformers C and D also do not match the experimental data as well as those for conformer A. For both conformers C and D, one calculated C=O stretch band is red shifted and one is blue shifted when compared to the experimental spectrum. The calculated structures for conformers C and D have only one carbonyl interacting with the sodium cation and the carboxyl carbonyl group does not interact with either the sodium cation or the phenyl group. Table 1 gives the calculated distances between the sodium cation and the oxygen atoms of the N-acetyl and carboxyl groups, indicative of the strength of electrostatic interaction.

With the scaling factor correction, the RMS differences between the experimental data and the calculated conformer C=O stretch frequencies are  $5\text{ cm}^{-1}$  for A,  $20\text{ cm}^{-1}$  for B,  $29\text{ cm}^{-1}$  for C

**Table 1**

Distance between sodium cation and oxygen atoms on the carbonyls of the carboxyl and on the N-acetyl functional groups for conformers A–D.

AcPhe conformer	Carboxyl carbonyl O	N-acetyl carbonyl O
Calculated distances (Angstroms) between sodium and oxygen atoms		
A	2.22	2.35
B	2.26	2.17
C	N/A	2.14
D	N/A	2.14

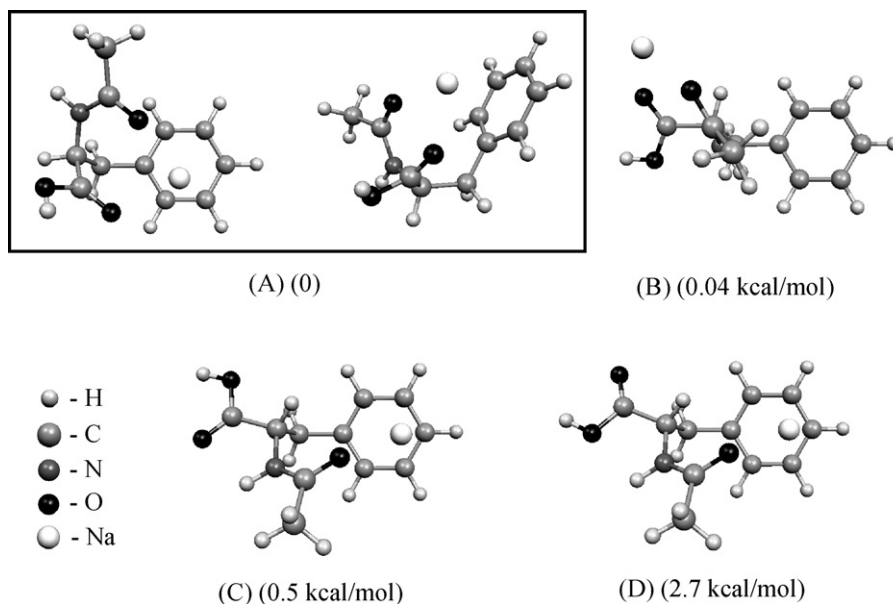


**Fig. 4.** Lowest energy conformers of sodiated AcPhe found from conformational search calculations. Relative energies were obtained at the B3LYP/6-31++G(d,p) level of theory and are zero-point energy corrected. An alternate view is included for conformer A to show the puckering of the structure.

and  $40\text{ cm}^{-1}$  for D, with frequency values for the experimental spectra taken from the peak maxima of the experimental bands. All other calculated bands for conformers C and D do not agree well with experimental data either (except that conformer D shows reasonable agreement with the bands at approximately  $1150$  and  $1525\text{ cm}^{-1}$ ). The observed IRMPD spectral bands can be assigned using the calculated results for conformer A (Fig. 6) although small contributions to the IRMPD spectrum from the other conformers are possible, due to the similar relative energies of the structures. Bands due to OH and NH bending motions would be expected to shift upon substitution of the labile H-atoms by a D-atom and are used extensively in the discussion of IRMPD spectra of H/D-exchanged AcPhe analogs below.

### 3.2. Hydrogen/deuterium exchange experiments

#### 3.2.1. AcPhe

For the solution-phase H/D exchange of AcPhe, the mass spectrum indicated that, as would be expected, two exchanges had taken place, one involving the amide hydrogen and one the carboxyl hydrogen. The IRMPD spectrum of sodiated AcPhe following solution-phase HDX is shown in Fig. 7.

In experiments involving gas-phase H/D exchange of sodiated AcPhe, the resultant mass spectra showed only a 1 Da mass increase, indicating that only one D for H substitution had occurred. An IRMPD spectrum of the singly deuterated complex ion was obtained and the calculated spectra for sodiated AcPhe with one D-substituted for either the amide or carboxyl hydrogen were com-

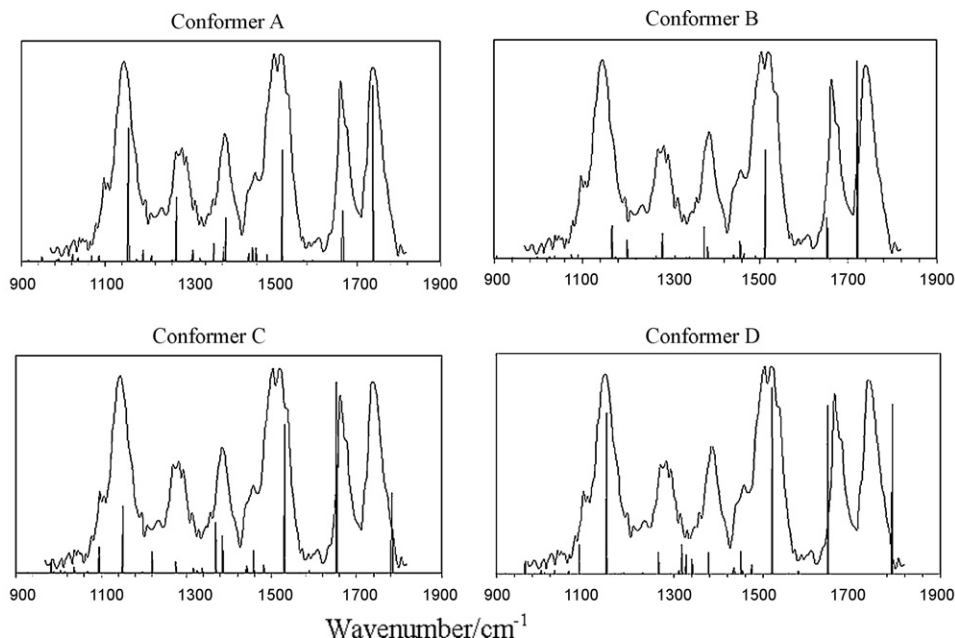


**Fig. 5.** Comparison of experimental IRMPD spectrum of  $\text{Na}^+\text{AcPhe}$  with calculated spectra (represented as sticks) of the theoretically determined lowest energy conformers A–D. Calculated vibrational frequencies are scaled by a factor of 0.965. For calculated spectra the ordinate is the single photon infrared intensity in  $\text{km/mol}$ . For the experimental IRMPD spectrum the ordinate is the IRMPD yield in arbitrary units scaled so that peak heights are comparable to those in the calculated spectra to assist in visual comparison.



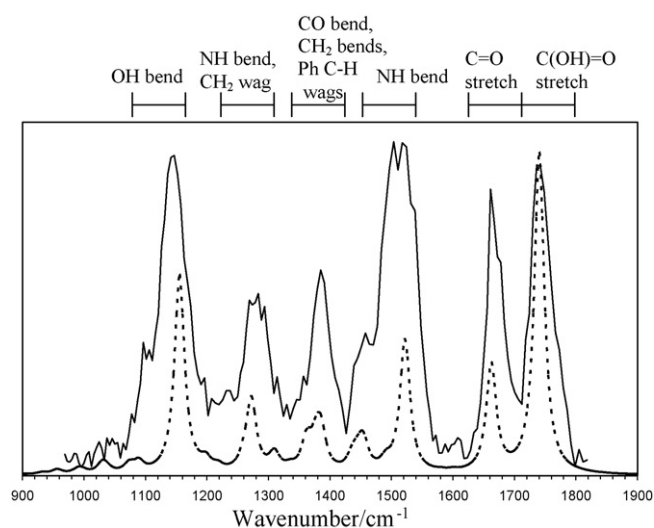


**Fig. 6.** Assignment of spectral bands in the IRMPD spectrum of sodiated AcPhe using calculated bands for conformer A. Calculated vibrational frequencies are scaled by a factor of 0.965 and the calculated spectrum has been convoluted with a  $20\text{ cm}^{-1}$  Gaussian profile. Ordinate values are as described for Fig. 5.

pared (Fig. 8). Agreement with the experimental spectrum is much better for the spectrum calculated for D exchange with the acidic hydrogen.

### 3.2.2. AcPheOMe

For sodiated AcPheOMe, no gas-phase H/D exchange was observed. AcPheOMe does not have a carboxyl hydrogen and exchange of the amide hydrogen is apparently quite slow in the gas phase (as was seen for sodium cation-attached AcPhe). One H/D exchange took place in solution-phase experiments, presumably at the amide hydrogen, as confirmed by the agreement between the IRMPD spectrum of mono-deuterated sodiated AcPheOMe and the calculated spectrum for the amide-deuterated species (Fig. 9A). The structure of this species is shown in Fig. 9C.

### 3.2.3. AcPheGlyOMe

Two exchanges of D for H were observed for AcPheGlyOMe in solution, and none in gas-phase experiments. This protected dipeptide has two amide hydrogens, and DFT calculations predict the most stable structure of the sodiated complex as shown in Fig. 9D. Agreement between the IRMPD spectrum of this doubly deuter-

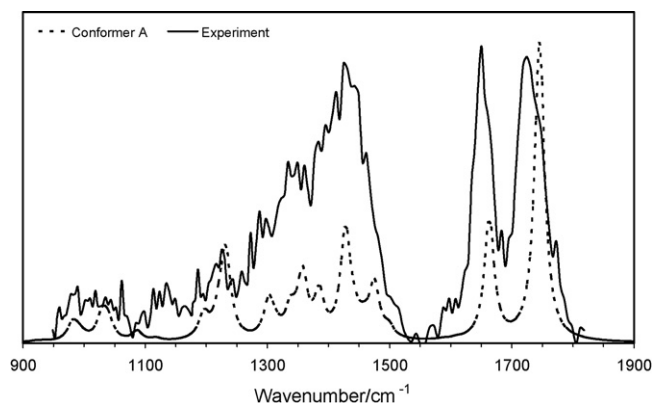


**Fig. 7.** IRMPD spectrum of sodiated AcPhe following solution-phase HDX (solid line) and calculated spectrum of the doubly deuterated conformer A (dashed line). D-atom substitution occurred at both the NH and COOH hydrogens. Calculated vibrational frequencies are scaled by a factor of 0.965. Ordinate values are as described for Fig. 5.

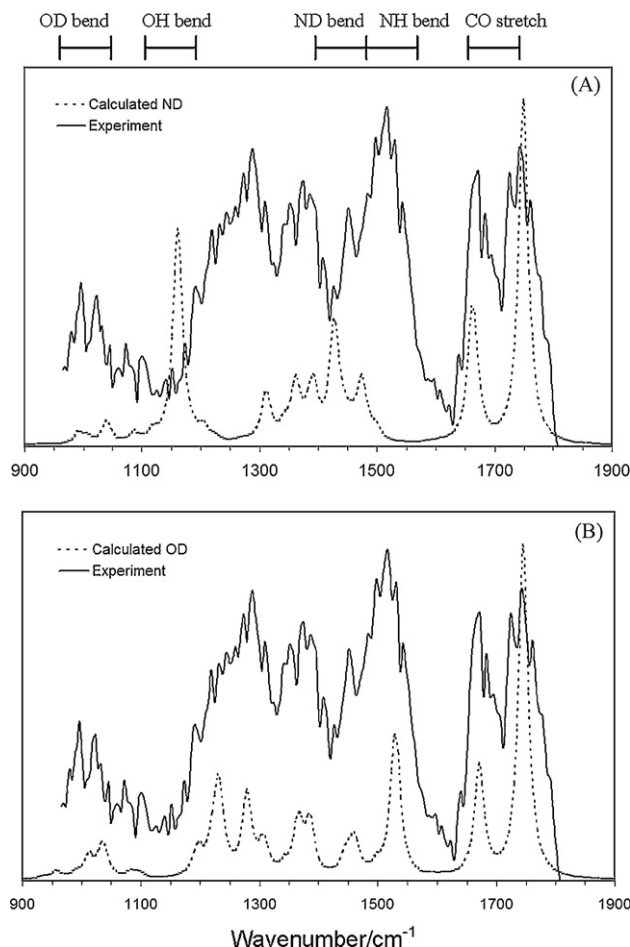


**Fig. 8.** Comparison of the singly deuterated sodiated AcPhe IRMPD spectrum with that of calculated conformer A if exchange had occurred at (A) the NH hydrogen or at (B) the COOH hydrogen. The wavelength range for relevant vibrational modes is indicated above spectrum (A). Calculated vibrational frequencies are scaled by a factor of 0.965. Ordinate values are as described for Fig. 5.

ated species and the calculated spectrum for the structure in Fig. 9D with both amide hydrogens exchanged is quite good (Fig. 9B). The most stable structures calculated for both sodiated AcPheOMe and AcPheGlyOMe involve interaction of the sodium cation with the phenyl ring and with the lone pairs on all carbonyl oxygens. Fig. 9C and D shows that these complexes have a puckered conformation.

Results for H/D exchange experiments involving the Phe analogs are summarized in Table 2. The results found in this study and others of phenylalanine indicate that the species behaves quite differently when interacting with a chelating metal, which seems to fix the structure into one conformation. Gas-phase H/D exchange has been observed for the amide hydrogen on other amino acids [63]. Direct substitution of the amide hydrogen with deuterium is slow, and earlier studies [1,64,65] indicate that if a hydroxyl group is available, the exchange will occur at the hydroxyl hydrogen fol-

**Table 2**

Summary of results from H/D exchange experiments, where no D for H substitution was observed for sodiated AcPheOMe and AcPheGlyOMe in the gas phase.

N-acetylphenylalanine species	Deuteration medium	Deuteration sites
Sodiated (AcPhe)	Gas phase	1 – OH
	Solution	2 – OH, NH
Sodiated (AcPheOMe)	Gas phase	None
	Solution	1 – NH
Sodiated (AcPheGlyOMe)	Gas phase	None
	Solution	2 – NH

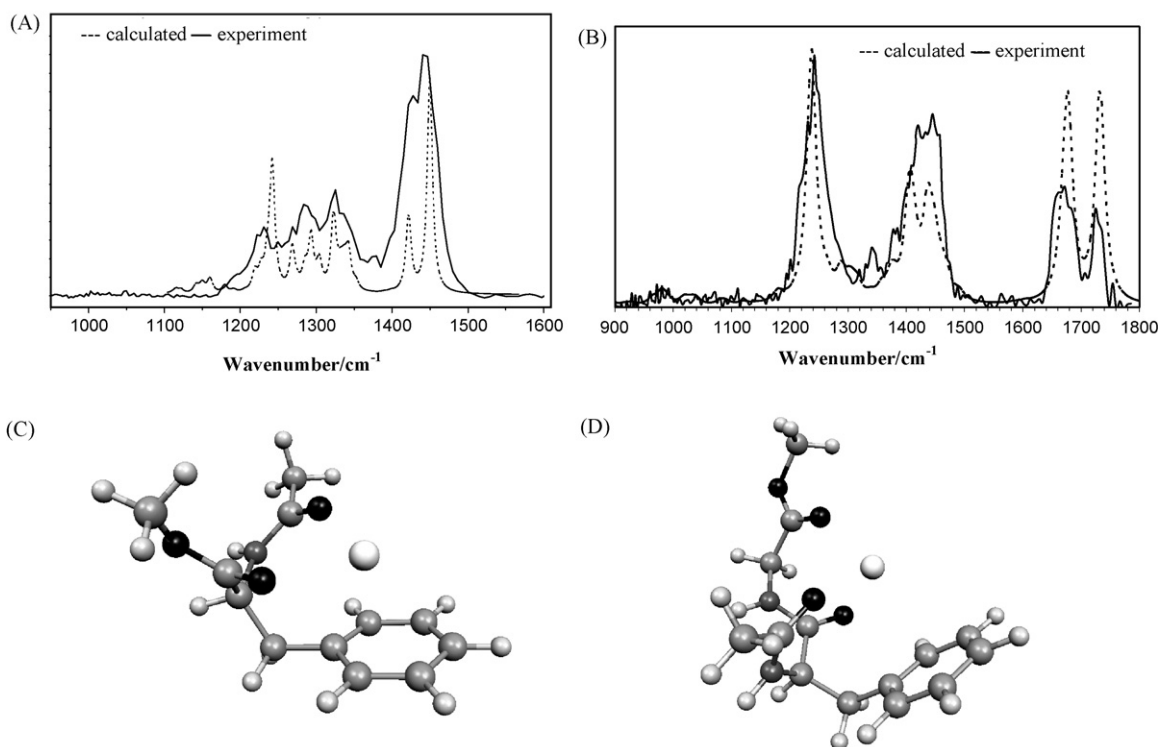


**Fig. 9.** Experimental IRMPD and calculated spectra for mono-deuterated sodiated AcPheOMe (A) and doubly deuterated sodiated AcPheGlyOMe (B). The lowest energy structures found are shown as (C) and (D), respectively. Calculated vibrational frequencies are scaled by a factor of 0.965. Ordinate values are as described for Fig. 5.

lowed by deuterium migration to the amide position. Formation of a chelated sodium cation complex apparently impedes migration of deuterium to the amide hydrogen, as seen for sodiated AcPhe, where exchange occurred at the carboxyl hydrogen but not at the amide hydrogen. In preliminary gas-phase H/D exchange experiments involving protonated (as opposed to sodiated) AcPhe, three hydrogen atoms were exchanged. Deuterium migration from the carboxyl group to the amide nitrogen was not impeded for this species.

### 3.3. Exchange kinetics

The rates of gas-phase H/D exchange were measured for both sodiated and protonated AcPhe ions reacting with ND<sub>3</sub>. Ion peak height versus time curves for the various undeuterated, singly deuterated, doubly deuterated and triply deuterated (the latter two for the protonated species only) ions were fit using the Kinetics program<sup>2</sup> and the pseudo-first order rate coefficients obtained from it were divided by the measured ND<sub>3</sub> pressure, corrected for ionization gauge sensitivity [66], to give the rates for each step of the HDX process.

For the single H/D exchange observed with sodiated AcPhe, a rate of  $1.53 \times 10^{-11}$  cm<sup>3</sup>/s was found. This is somewhat less than the slowest H/D exchange rates reported previously [11] for ND<sub>3</sub> reacting with protonated glycine oligomers and comparable to the slower rates seen [67] for CD<sub>3</sub>OD and D<sub>2</sub>O reacting with several protonated amino acids and O-methylated amino acids. The ionization gauge used in this work was not calibrated versus a capacitance manometer, and was located some distance from the FTICR analyzer cell. Thus the true pressure in the cell might well have differed considerably from that read on the gauge, in part explaining the discrepancy between our rate for ND<sub>3</sub> exchange and those reported

previously [11]. It is also possible that the puckered conformation of the sodiated AcPhe and the presence of a sodium ion rather than a proton could slow the rate of H/D exchange.

In the HDX experiments involving protonated AcPhe, continuous ejection of the singly deuterated ion did not totally eliminate production of doubly and triply deuterated species. Therefore some collisions of ND<sub>3</sub> with protonated AcPhe result in exchange of two deuterium atoms, as reported previously [11] for ND<sub>3</sub> reacting with protonated glycine oligomers. The mechanism used in the Kinetics program to fit the ion peak height versus time curves included not only single deuteration reactions, but this double deuteration reaction as well. Rates for double deuteration of the singly deuterated ion and triple deuteration of the undeuterated ion were quite slow and were not included in the mechanism used to fit the data. The rate coefficients obtained for the four reactions used to fit the data (again using an ionization gauge sensitivity corrected for ammonia) were  $k_{0 \rightarrow 1} = 3.6 \times 10^{-11}$  cm<sup>3</sup>/s,  $k_{1 \rightarrow 2} = 3.5 \times 10^{-11}$  cm<sup>3</sup>/s,  $k_{2 \rightarrow 3} = 2.0 \times 10^{-11}$  cm<sup>3</sup>/s, and  $k_{0 \rightarrow 2} = 2.0 \times 10^{-11}$  cm<sup>3</sup>/s, where the subscripts on the rate coefficients indicate the number of deuterium atoms in the ion. No experiments were undertaken to assess the rates of back exchange, which would make the rates of gas-phase HDX reported here less than the true rates. Thus the rate coefficients given above should be considered lower limits to the true values for gas-phase HDX.

### 4. Conclusions

Shifts of vibrational spectral bands upon H/D exchange with sodiated phenylalanine analogs have been predicted theoretically and compared to those observed in gas-phase infrared multiple photon dissociation spectra. The H/D exchange experiments not only provided band assignment confirmation, but simultaneously helped identify structural features of the Phe analogs. Structural characteristics common to all phenylalanine analogs in this study include:

<sup>2</sup> D.E. Richardson, personal communication, University of Florida, 2009.

- The calculated lowest energy structures for all three analogs include cation– $\pi$  interactions.
- Torsion of carbonyls toward the phenyl ring, in order to interact with the sodium cation, causes the conformation to stay relatively rigid and in a puckered state.
- Amide group hydrogens are found to be non-labile for H/D exchange in the sodium-chelated phenylalanine analogs studied in this work.

It is apparent that for the systems discussed here the amide hydrogen is not labile to gas-phase HDX, in contrast to results seen for many protonated peptides in the gas phase, where HDX can be observed for amide hydrogens [1,67]. This is most likely due to the fact that for the sodiated species studied here sodium binding competes with H-bonding; and H-bonding is essential in any H/D exchange reaction mechanism (relay or others).

## Acknowledgements

The authors would like to thank the FELIX staff for their skillful assistance. Funding was provided by the National Science Foundation (OISE-0730072 and CHE-0718007) and the NSF-supported National High Field FTICR Facility at the National High Magnetic Field Laboratory for FTICR construction and transportation to The Netherlands. This work is part of the research program of FOM, which is financially supported by the Nederlandse Organisatie voor Wetenschappelijk Onderzoek.

## References

- [1] M.K. Green, C.B. Lebrilla, Ion-molecule reactions as probes of gas-phase structures of peptides and proteins, *Mass Spectrom. Rev.* 16 (1997) 53–71.
- [2] S.J. Valentine, D.E. Clemmer, H/D exchange levels of shape-resolved cytochrome c conformers in the gas phase, *J. Am. Chem. Soc.* 119 (1997) 3558–3566.
- [3] F.W. McLafferty, Z.Q. Guan, U. Haupts, T.D. Wood, N.L. Kelleher, Gaseous conformational structures of cytochrome c, *J. Am. Chem. Soc.* 120 (1998) 4732–4740.
- [4] M.A. Freitas, A.G. Marshall, Rate and extent of gas-phase hydrogen/deuterium exchange of bradykinins: evidence for peptide zwitterions in the gas phase, *Int. J. Mass Spectrom.* 183 (1999) 221–231.
- [5] L. Konermann, D.A. Simmons, Protein-folding kinetics and mechanisms studied by pulse-labeling and mass spectrometry, *Mass Spectrom. Rev.* 22 (2003) 1–26.
- [6] J.C. Jurchen, R.E. Cooper, E.R. Williams, The role of acidic residues and of sodium ion adduction on the gas-phase H/D exchange of peptides and peptide dimers, *J. Am. Soc. Mass Spectrom.* 14 (2003) 1477–1487.
- [7] T. Wytenbach, B. Paizs, P. Barran, L. Breci, D.F. Liu, S. Suhai, V.H. Wysocki, M.T. Bowers, The effect of the initial water of hydration on the energetics, structures, and H/D exchange mechanism of a family of pentapeptides: an experimental and theoretical study, *J. Am. Chem. Soc.* 125 (2003) 13768–13775.
- [8] J. Atzrodt, V. Derdau, T. Fey, J. Zimmermann, The renaissance of H/D exchange, *Angew. Chem. Int. Ed.* 46 (2007) 7744–7765.
- [9] T.E. Wales, J.R. Engen, Hydrogen exchange mass spectrometry for the analysis of protein dynamics, *Mass Spectrom. Rev.* 25 (2006) 158–170.
- [10] A. Kohen, H.-H. Limbach (Eds.), *Isotope Effects in Chemistry and Biology*, CRC Press LLC, Boca Raton, 2006.
- [11] S. Campbell, M.T. Rodgers, E.M. Marzluff, J.L. Beauchamp, Deuterium exchange reactions as a probe of biomolecule structure. Fundamental studies of gas-phase H/D exchange reactions of protonated glycine oligomers with D<sub>2</sub>O, CD<sub>3</sub>OD, CD<sub>3</sub>CO<sub>2</sub>D, and ND<sub>3</sub>, *J. Am. Chem. Soc.* 117 (1995) 12840–12854.
- [12] G.E. Reid, R.A.J. O'Hair, M.L. Styles, W.D. McFadyen, R.J. Simpson, Gas phase ion-molecule reactions in a modified ion trap: H/D exchange of non-covalent complexes and coordinatively unsaturated platinum complexes, *Rapid Commun. Mass Spectrom.* 12 (1998) 1701–1708.
- [13] D.M. Peiris, M.A. Cheeseman, R. Ramanathan, J.R. Eyler, Infrared multiple-photon dissociation spectra of gaseous-ions, *J. Phys. Chem.* 97 (1993) 7839–7843.
- [14] R.C. Dunbar, Photodissociation of trapped ions, *Int. J. Mass Spectrom.* 200 (2000) 571–589.
- [15] J. Oomens, B.G. Sartakov, G. Meijer, G. Von Helden, Gas-phase infrared multiple photon dissociation spectroscopy of mass-selected molecular ions, *Int. J. Mass Spectrom.* 254 (2006) 1–19.
- [16] J.S. Brodbelt, J.J. Wilson, Infrared multiphoton dissociation in quadrupole ion traps, *Mass Spectrom. Rev.* 28 (2009) 390–424.
- [17] N.C. Polfer, J. Oomens, Vibrational spectroscopy of bare and solvated ionic complexes of biological relevance, *Mass Spectrom. Rev.* 28 (2009) 468–494.
- [18] J.R. Eyler, Infrared multiple photon dissociation spectroscopy of ions in Penning traps, *Mass Spectrom. Rev.* 28 (2009) 448–467.
- [19] Y.P. Ho, Y.C. Yang, S.J. Klippenstein, R.C. Dunbar, Infrared spectral properties of the naphthalene cation – radiative cooling kinetics experiments and density-functional calculations, *J. Phys. Chem.* 99 (1995) 12115–12124.
- [20] D.M. Peiris, J.M. Riveros, J.R. Eyler, Infrared multiple photon dissociation spectra of methanol-attached anions and proton-bound dimer cations, *Int. J. Mass Spectrom. Ion Process.* 159 (1996) 169–183.
- [21] D.M. Peiris, Y.J. Yang, R. Ramanathan, K.R. Williams, C.H. Watson, J.R. Eyler, Infrared multiphoton dissociation of electrosprayed crown ether complexes, *Int. J. Mass Spectrom. Ion Process.* 158 (1996) 365–378.
- [22] D.T. Moore, J. Oomens, L. van der Meer, G. von Helden, G. Meijer, J. Valle, A.G. Marshall, J.R. Eyler, Probing the vibrations of shared, OH+O-bound protons in the gas phase, *ChemPhysChem* 5 (2004) 740–743.
- [23] J.J. Valle, J.R. Eyler, J. Oomens, D.T. Moore, A.F.G. van der Meer, G. von Helden, G. Meijer, C.L. Hendrickson, A.G. Marshall, G.T. Blakney, Free electron laser-Fourier transform ion cyclotron resonance mass spectrometry facility for obtaining infrared multiphoton dissociation spectra of gaseous ions, *Rev. Sci. Instrum.* 76 (2005) 0231031–0231037.
- [24] D.T. Moore, J. Oomens, J.R. Eyler, G. von Helden, G. Meijer, R.C. Dunbar, Infrared spectroscopy of gas-phase Cr<sup>+</sup> coordination complexes: determination of binding sites and electronic states, *J. Am. Chem. Soc.* 127 (2005) 7243–7254.
- [25] G. Wu, A.J. Stace, IRMPD study of the furan cation in an ion trap: evidence of the extreme effect a competitive shift can have on reaction pathway, *Chem. Phys. Lett.* 412 (2005) 1–4.
- [26] R.C. Dunbar, D.T. Moore, J. Oomens, IR-spectroscopic characterization of acetophenone complexes with Fe<sup>+</sup>, Co<sup>+</sup>, and Ni<sup>+</sup> using free-electron-laser IRMPD, *J. Phys. Chem. A* 110 (2006) 8316–8326.
- [27] J. Szczepanski, H.Y. Wang, M. Vala, A.G.G.M. Tielens, J.R. Eyler, J. Oomens, Infrared spectroscopy of gas-phase complexes of Fe<sup>+</sup> and polycyclic aromatic hydrocarbon molecules, *Astrophys. J.* 646 (2006) 666–680.
- [28] J. Oomens, N. Polfer, D.T. Moore, L. van der Meer, A.G. Marshall, J.R. Eyler, G. Meijer, G. von Helden, Charge-state resolved mid-infrared spectroscopy of a gas-phase protein, *Phys. Chem. Chem. Phys.* 7 (2005) 1345–1348.
- [29] N.C. Polfer, J. Oomens, R.C. Dunbar, IRMPD spectroscopy of metal-ion/tryptophan complexes, *Phys. Chem. Chem. Phys.* 8 (2006) 2744–2751.
- [30] N.C. Polfer, J. Oomens, R.C. Dunbar, Alkali metal complexes of the dipeptides PheAla and AlaPhe: IRMPD spectroscopy, *ChemPhysChem* 9 (2008) 579–589.
- [31] N.C. Polfer, R.C. Dunbar, J. Oomens, Observation of zwitterion formation in the gas-phase H/D-exchange with CH<sub>3</sub>OD: solution-phase structures in the gas phase, *J. Am. Soc. Mass Spectrom.* 18 (2007) 512–516.
- [32] Z.X. Tian, A. Pawlow, J.C. Poutsma, S.R. Kass, Are carboxyl groups the most acidic sites in amino acids? Gas-phase acidity, H/D exchange experiments, and computations on cysteine and its conjugate base, *J. Am. Chem. Soc.* 129 (2007) 5403–5407.
- [33] L.C. Snoek, E.G. Robertson, R.T. Kroemer, J.P. Simons, Conformational landscapes in amino acids: infrared and ultraviolet ion-dip spectroscopy of phenylalanine in the gas phase, *Chem. Phys. Lett.* 321 (2000) 49–56.
- [34] R.C. Dunbar, Complexation of Na<sup>+</sup> and K<sup>+</sup> to aromatic amino acids: a density functional computational study of cation– $\pi$  interactions, *J. Phys. Chem. A* 104 (2000) 8067–8074.
- [35] V. Ryzhov, R.C. Dunbar, B. Cerda, C. Wesdemiotis, Cation– $\pi$  effects in the complexation of Na<sup>+</sup> and K<sup>+</sup> with Phe, Tyr, and Trp in the gas phase, *J. Am. Soc. Mass Spectrom.* 11 (2000) 1037–1046.
- [36] A. Gapeev, R.C. Dunbar, Cation– $\pi$  interactions and the gas-phase thermochemistry of the Na<sup>+</sup>/phenylalanine complex, *J. Am. Chem. Soc.* 123 (2001) 8360–8365.
- [37] C.H. Ruan, M.T. Rodgers, Cation– $\pi$  interactions: structures and energetics of complexation of Na<sup>+</sup> and K<sup>+</sup> with the aromatic amino acids, phenylalanine, tyrosine, and tryptophan, *J. Am. Chem. Soc.* 126 (2004) 14600–14610.
- [38] N.C. Polfer, J. Oomens, D.T. Moore, G. von Helden, G. Meijer, R.C. Dunbar, Infrared spectroscopy of phenylalanine Ag(I) and Zn(II) complexes in the gas phase, *J. Am. Chem. Soc.* 128 (2006) 517–525.
- [39] G. von Helden, I. Compagnon, M.N. Blom, M. Frankowski, U. Erlekam, J. Oomens, B. Brauer, R.B. Gerber, G. Meijer, Mid-IR spectra of different conformers of phenylalanine in the gas phase, *Phys. Chem. Chem. Phys.* 10 (2008) 1248–1256.
- [40] E.G. Robertson, J.P. Simons, Getting into shape: conformational and supramolecular landscapes in small biomolecules and their hydrated clusters, *Phys. Chem. Chem. Phys.* 3 (2001) 1–18.
- [41] J.B. Fenn, M. Mann, C.K. Meng, S.F. Wong, C.M. Whitehouse, Electrospray ionization for mass-spectrometry of large biomolecules, *Science* 246 (1989) 64–71.
- [42] J.B. Fenn, M. Mann, C.K. Meng, S.F. Wong, C.M. Whitehouse, Electrospray ionization-principles and practice, *Mass Spectrom. Rev.* 9 (1990) 37–70.
- [43] R.B. Cole (Ed.), *Electrospray Ionization Mass Spectrometry: Fundamentals, Instrumentation, and Applications*, Wiley, New York, 1997.
- [44] P. Hohenberg, W. Kohn, Inhomogeneous electron gas, *Phys. Rev. B* 136 (1964) B864–B871.
- [45] W. Kohn, L.J. Sham, Self-consistent equations including exchange and correlation effects, *Phys. Rev.* 140 (1965) A1133–A1138.
- [46] W. Koch, M.C. Holthausen, *A Chemist's Guide to Density Functional Theory*, 2nd ed., Wiley, Chichester, 2001.
- [47] A.G. Marshall, T.C.L. Wang, T.L. Ricca, Tailored excitation for Fourier-transform ion-cyclotron resonance mass-spectrometry, *J. Am. Chem. Soc.* 107 (1985) 7893–7897.
- [48] L. Chen, A.G. Marshall, Effect of time-domain dynamic range on stored waveform excitation for Fourier transform ion cyclotron resonance mass spectrometry, *Rapid Commun. Mass Spectrom.* 1 (1987) 39–42.

- [49] L. Chen, T.C.L. Wang, T.L. Ricca, A.G. Marshall, Phase-modulated stored wave-form inverse Fourier-transform excitation for trapped ion mass-spectrometry, *Anal. Chem.* 59 (1987) 449–454.
- [50] S.H. Guan, A.G. Marshall, Stored wave-form inverse Fourier-transform axial excitation/ejection for quadrupole ion-trap mass-spectrometry, *Anal. Chem.* 65 (1993) 1288–1294.
- [51] S.H. Guan, A.G. Marshall, Stored waveform inverse Fourier transform (SWIFT) ion excitation in trapped-ion mass spectrometry: theory and applications, *Int. J. Mass Spectrom. Ion Process.* 158 (1996) 5–37.
- [52] D. Oepts, A.F.G. Vandermeer, P.W. Vanamersfoort, The free-electron-laser user facility FELIX, *Infrared Phys. Technol.* 36 (1995) 297–308.
- [53] T.G.A. Verhoeven, W.A. Bongers, V.L. Bratman, M. Caplan, G.G. Denisov, C.A.J. Van der Geer, P. Manintveld, A.J. Poelman, J. Plomp, A.V. Savilov, P.H.M. Smeets, A.B. Sterk, W.H. Urbanus, First mm-wave generation in the FOM free electron maser, *IEEE Trans. Plasma Sci.* 27 (1999) 1084–1091.
- [54] HyperChem(TM) Professional 7.51, Hypercube, Inc., 2007.
- [55] F.A. Momany, R.F. McGuire, A.W. Burgess, H.A. Scheraga, Energy parameters in polypeptides. 7. Geometric parameters, partial atomic charges, nonbonded interactions, hydrogen-bond interactions, and intrinsic torsional potentials for naturally occurring amino-acids, *J. Phys. Chem.* 79 (1975) 2361–2381.
- [56] L.G. Dunfield, A.W. Burgess, H.A. Scheraga, Energy parameters in polypeptides. 8. Empirical potential-energy algorithm for conformational-analysis of large molecules, *J. Phys. Chem.* 82 (1978) 2609–2616.
- [57] G. Chang, W.C. Guida, W.C. Still, An internal coordinate Monte-Carlo method for searching conformational space, *J. Am. Chem. Soc.* 111 (1989) 4379–4386.
- [58] M.J. Frisch, G.W. Trucks, H.B. Schlegel, G.E. Scuseria, M.A. Robb, J.R. Cheeseman, J.A. Montgomery Jr., T. Vreven, K.N. Kudin, J.C. Burant, J.M. Millam, S.S. Iyengar, J. Tomasi, V. Barone, B. Mennucci, M. Cossi, G. Scalmani, N. Rega, G.A. Petersson, H. Nakatsuji, M. Hada, M. Ehara, K. Toyota, R. Fukuda, J. Hasegawa, M. Ishida, T. Nakajima, Y. Honda, O. Kitao, H. Nakai, M. Klene, X. Li, J.E. Knox, H.P. Hratchian, J.B. Cross, V. Bakken, C. Adamo, J. Jaramillo, R. Gomperts, R.E. Stratmann, O. Yazyev, A.J. Austin, R. Cammi, C. Pomelli, J.W. Ochterski, P.Y. Ayala, K. Morokuma, G.A. Voth, P. Salvador, J.J. Dannenberg, V.G. Zakrzewski, S. Dapprich, A.D. Daniels, M.C. Strain, O. Farkas, D.K. Malick, A.D. Rabuck, K. Raghavachari, J.B. Foresman, J.V. Ortiz, Q. Cui, A.G. Baboul, S. Clifford, J. Cioslowski, B.B. Stefanov, G. Liu, A. Liashenko, P. Piskorz, I. Komaromi, R.L. Martin, D.J. Fox, T. Keith, M.A. Al-Laham, C.Y. Peng, A. Nanayakkara, M. Challacombe, P.M.W. Gill, B. Johnson, W. Chen, M.W. Wong, C. Gonzalez, J.A. Pople, Gaussian 03 Version 02 ed., Gaussian, Inc., Wallingford CT, 2004.
- [59] P.C. Hariharan, J.A. Pople, Influence of polarization functions on MO hydrogenation energies, *Theor. Chim. Acta* 28 (1973) 213–222.
- [60] V.A. Rassolov, J.A. Pople, M.A. Ratner, T.L. Windus, 6-31G\* basis set for atoms K through Zn, *J. Chem. Phys.* 109 (1998) 1223–1229.
- [61] W.J. Hehre, R. Ditchfie, J.A. Pople, Self-consistent molecular-orbital methods. 12. Further extensions of Gaussian-type basis sets for use in molecular-orbital studies of organic-molecules, *J. Chem. Phys.* 56 (1972) 2257–2261.
- [62] T. Clark, J. Chandrasekhar, G.W. Spitznagel, P.V. Schleyer, Efficient diffuse function-augmented basis-sets for anion calculations. 3. The 3-21+G basis set for 1st-row elements, Li–F, *J. Comp. Chem.* 4 (1983) 294–301.
- [63] N.N. Dookeran, A.G. Harrison, Reactive collisions in quadrupole cells. Part 4. Gas-phase H–D exchange reactions of protonated amino acids and peptides with ND<sub>3</sub>, *J. Mass Spectrom.* 30 (1995) 666–674.
- [64] E. Gard, D. Willard, J. Bregar, M.K. Green, C.B. Lebrilla, Site-specificity in the H–D exchange-reactions of gas-phase protonated amino-acids with CH<sub>3</sub>OD, *Org. Mass Spectrom.* 28 (1993) 1632–1639.
- [65] M.K. Green, C.B. Lebrilla, The role of proton-bridged intermediates in promoting hydrogen–deuterium exchange in gas-phase protonated diamines, peptides and proteins, *Int. J. Mass Spectrom.* 175 (1998) 15–26.
- [66] J.E. Bartmess, R.M. Georgiadis, Empirical-methods for determination of ionization gauge relative sensitivities for different gases, *Vacuum* 33 (1983) 149–153.
- [67] M. Rozman, The gas-phase H/D exchange mechanism of protonated amino acids, *J. Am. Soc. Mass Spectrom.* 16 (2005) 1846–1852.